

# A 2D Model of a Triple Layer Electromagnetic Heat Exchanger with Porous Media Flow

Ajit A. Mohekar<sup>1</sup>, Burt S. Tilley<sup>1,2</sup>, and Vadim V. Yakovlev<sup>2</sup>

<sup>1</sup>Department of Mechanical Engineering, Worcester Polytechnic Institute, MA, USA

<sup>2</sup>Department of Mathematical Sciences, Center for Industrial Mathematics and Statistics, Worcester Polytechnic Institute, MA, USA

aamohekar@wpi.edu, tilley@wpi.edu, vadim@wpi.edu

**Abstract**— Electromagnetic heat exchangers are complex devices involving multiple physical processes and requiring extensive experimental developments. Effectiveness of their operation means efficient conversion of electromagnetic energy into useful mechanical work. In this paper, we present a 2D numerical model of a porous-media-based electromagnetic heat exchanger with three layers. We first report a double S- power response curve when no fluid flow is considered. Comparing the developed curve with the one produced by analytical approach, we find both the curves in satisfactory agreement. After validation, we introduce Darcy's flow in porous medium, and calculate the power absorbed by the fluid and overall thermal efficiency of the heat exchanger. It is shown that the net power absorbed by the coolant flowing in the porous media is mainly dependent on fluid velocity and outlet temperature. When operating on the middle branch of the double S-curve, total thermal energy collected by the fluid is high, but overall thermal efficiency of the device is low because of the slow movement of the fluid.

**Keywords**— computational modeling, electromagnetic heating, porous media flow, thermal runaway

## I. INTRODUCTION

High power electromagnetic heat exchangers (EMHE) have potential applications in wireless energy transmissions [1], beamed energy propulsion [2], [3], and other emerging technologies. The key function of EMHEs is to efficiently convert electromagnetic (EM) energy into useful mechanical work. Operations of EMHEs depend on the combined effects of electromagnetic, heat transfer and fluid flow phenomena, and require particularly extensive experimental developments. Therefore, the design of effective EMHEs demands multi-physics models that are capable of adequately simulating all essential effects occurring in EMHEs.

The loss factor of an absorbing material leads to its heating during EM irradiation. When the loss factor increases exponentially with temperature, the EM losses increase, which may result in the event of *thermal runaway*. The phenomenon of thermal runaway for ceramic materials was studied experimentally [4], [5], numerically [6], and analytically [7].

Equilibrium of EM heating can be represented with a *power response curve* which is a parametric plot of the average steady-state temperature as a function of the applied power. For an incident EM wavelength much larger than the layer's thickness, analytical models of EM heating of laminate structures [7]–[9] reported an S-shaped power response curve. The lower branch of the S-curve has very low stable temperatures,

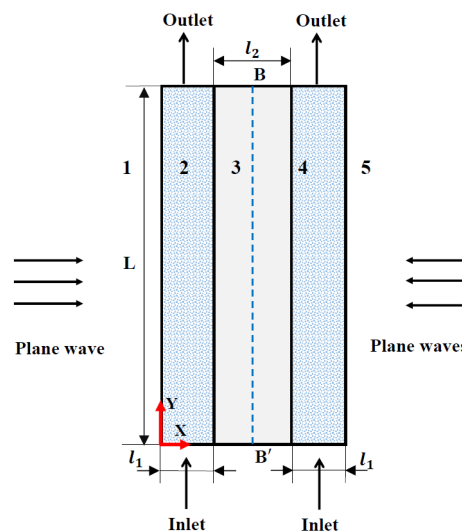


Fig. 1. Geometry of considered triple layer heat exchanger undergoing symmetric (about  $BB'$ ) irradiation by plane waves. Layers 1 and 5 are free space, 2 and 4 are lossless porous media, and 3 is a lossy ceramic material.

so EMHEs operating in this region may be inefficient, and upper branch may have very high stable temperatures (up to 1500- 2000 K) because of thermal runaway. Such high temperatures can damage the materials through melting or mechanical failure. In the triple layer laminate (lossless-lossy-lossless) structure, when the wavelength is comparable to the layer's thickness, electric field resonance may be achieved in the lossy layer; that allows the S-curve to acquire another (middle) stable branch and become the double S-curve [10]. This new middle branch may have temperatures on the order of 1000 K, which makes this region favorable for EMHE operations.

The model [11] verified existence of the double S-curve numerically for a triple layer laminate structure. This model did not consider actual materials, but assumed the media to have a very small volumetric heat capacity. Also, a numerical model of the triple layer EMHE with a fully developed Poiseuille flow as a coolant with a small Reynolds number was developed in [12]. It was shown that the thermal efficiency of considered EMHE may be dramatically increased when it operates on the middle branch of the double S-curve.

Table 1. Material Properties of the media in the setup in Fig. 1

Medium (Region)	$\epsilon_r$	$\sigma(T)$ [S/m]	$k$ [W/m · K]	$\rho C_p$ [J/m <sup>3</sup> K]	$\nu$ [Pa · s]
Free Space (1,5)	1	0	-	-	-
Lossless porous medium (2,4)	42	0	0.42	$2.6 \times 10^6$	0.001
Ceramic material (Zirconia) (3) [6]	6.69	$0.0009e^{2.72[\frac{T-300}{300}]}$	0.198	$0.6 \times 10^6$	-

Another approach for collecting thermal energy may include consideration of fluid (coolant) flow through a porous medium. To the best of our knowledge, numerical models describing operations of EMHEs with porous media flow as a mean of collecting thermal energy have not been reported yet.

In this paper, we consider a setup shown in Fig. 1 with zirconia as lossy ceramic layer in region 3, and lossless porous medium with zirconia as matrix (or skeleton) portion and a fluid as pore portion in region 2 and 4. We extend the numerical model [11], and describe the nature of the power response curve for the considered structure when no fluid flow is considered in region 2 and 4. To validate the model we compare the computed power response curve with the one produced by the analytical approach of [10].

After validation, we allow a lossless fluid to flow through the porous medium in regions 2 and 4. We assume that the fluid is incompressible and its motion is governed by the Darcy's law to better classify the phenomena in a more realistic scenario. We visualize steady-state temperature profiles, calculate the power density collected by the fluid, and also discuss the overall thermal efficiency of the EMHE. Finally, we demonstrate the effect of inlet fluid pressure on the steady-state temperature profiles and efficiency.

## II. NUMERICAL MODEL

We consider a triple layer laminate structure as shown in Fig. 1. Incoming plane wave with frequency ( $f$ ) of 2.45 GHz is assumed to be polarized along the Z-direction and traveling along the X-direction. The incident power density of the EM waves is given as

$$P_{av} = E_0^2 / 2\eta,$$

where  $E_0$  is amplitude of the incident EM waves and  $\eta$  is the characteristic impedance of free space. In order to achieve an electric field resonance in the lossy layer (region 3), we choose geometrical parameters of the structure according to the resonance criteria [10]

$$l_1 = \frac{n_1 \lambda_2}{4}, \text{ and } l_2 = \frac{n_2 \lambda_3}{2},$$

where  $n_1$  and  $n_2$  are any odd numbers,  $\lambda_2$  and  $\lambda_3$  are wavelength in region 2 and 3, respectively. For the considered geometry, we take  $n_1 = 3$  and  $n_2 = 1$ , and  $L = 10l_2$ .

### A. Governing Equations

We develop a numerical model in COMSOL Multiphysics which solves nonlinear coupled system of equations:

$$\nabla^2 \vec{E}_j + k_0^2 \mu_{rj} \left[ \epsilon_{rj} - i \frac{\sigma_j(T_j)}{\omega \epsilon_0} \right] \vec{E}_j = 0, \quad (1)$$

$$\nabla \cdot \vec{V}_j = 0, \quad (2)$$

$$\vec{V}_j = -\frac{\psi}{\nu} \nabla P_j \quad (3)$$

$$(\rho c_p)_{mj} \frac{\partial T_j}{\partial t} + (\rho c_p)_{fj} \vec{V}_j \cdot \nabla T = k_j \nabla^2 T_j + \frac{1}{2} \sigma_j(T_j) |E_j|^2, \quad (4)$$

where  $\vec{E}$  is electric field;  $k_0$  is wave number of free space;  $\mu_r$  and  $\epsilon_r$  are relative permeability and permittivity, respectively;  $T$  is temperature;  $\sigma$  is effective electrical conductivity;  $\omega$  is angular frequency;  $\epsilon_0$  is permittivity of free space;  $\rho$  is density;  $\vec{V}$  is velocity of fluid;  $P$  is fluid pressure;  $\psi$  is permeability of the porous medium;  $\nu$  is dynamic viscosity;  $c_p$  is specific heat capacity; and  $k$  is thermal conductivity;  $(\rho c_p)_m$  and  $(\rho c_p)_f$  are effective volumetric heat capacity of porous and fluid media, respectively; if the material is non porous,  $(\rho c_p)_m = (\rho c_p)_f$ . Subscript  $j$  represents region of the solution.

We solve (1) for  $j = 1, \dots, 5$ ; (2), (3) for  $j = 2, 4$ ; (4) for  $j = 2, 3, 4$ . For the first model in absence of fluid flow,  $\vec{V}_j = 0$  for  $j = 2, 3, 4$ . When Darcy flow is considered in region 2 and 4,  $\vec{V}_2, \vec{V}_4$  are non-zero and  $\vec{V}_3$  is zero, and gauge pressures at the inlet and outlet were assumed to be constants, and pressure gradient along X-direction was assumed to be zero (i.e. fluid only flows along positive Y-direction). In both models, the top and bottom boundaries of region 2, 3, and 4 are assumed to be thermally insulated; we set normal component of gradient of the electric field to be zero at the top and bottom boundaries of region 2, 3, and 4; a symmetry condition is applied at  $BB'$ ; boundaries between region 1 and 2, 4 and 5 are exposed to ambient temperature of 300 K with heat transfer coefficient  $h = 8.84 \text{ W/m}^2 \text{ K}$  undergoing Newton's law of cooling. We also define the Biot number as  $Bi = hl_1/k_{2,4}$ .

### B. Assumptions

We consider material properties of the layered structure as given in Table 1. All the materials used are assumed to be non-magnetic ( $\mu_r = 1$ ). Only the middle layer (region 3) absorbs EM energy; the outer layers (regions 1, 2, 4, and 5) are considered lossless. The effective electrical conductivity of zirconia is assumed to be temperature dependent; all other thermal and dielectric properties are temperature independent. Effective thermal properties and  $\epsilon_r$  for the porous medium are calculated based on mixture theory [13], [14] as

$$\xi_m = \theta \xi_f + (1 - \theta) \xi_s, \quad (5)$$

where  $\theta$  is porosity of the medium,  $\xi$  is any material parameter ( $\rho C_p$ ,  $k$ , or  $\epsilon_r$ ), and,  $f$  and  $s$  denote fluid and solid portions of the porous medium, respectively. In both the models, we assume that porosity and permeability are both independent of each other, and  $\theta = 0.55$  and  $\psi = 2.8 \times 10^{-10}$ . The

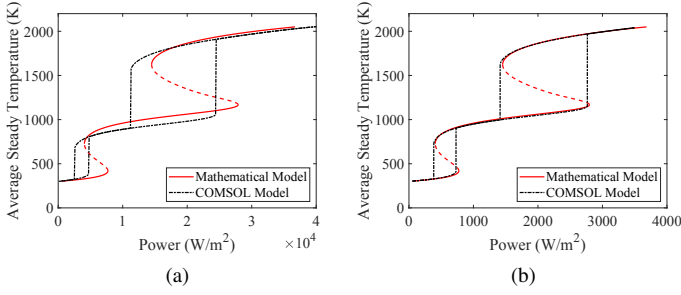


Fig. 2. Comparison of the double S-curves produced by the COMSOL model and the mathematical approach [10] for  $Bi = 0.3$  (a)  $Bi = 0.03$  (b).

resulting material properties of the considered porous medium are mentioned in the Table 1.

### C. Mesh, Solver, and Convergence Criteria

We use quadratic Lagrange triangular elements to spatially discretize the geometry, and determine maximum size of the element according to the meshing criteria discussed in [11]. Also, due to a high degree of nonlinearity, we use COMSOL's adaptive time-dependent solver and steady-state is assumed to be reached when an absolute difference between average temperatures at previous and current time step falls below  $10^{-4}$ . The adaptive time-dependent solver discretizes temporal gradients using second order backward difference method. Since volumetric heat capacity of the considered materials is very high, it took approximately  $10^5$  time steps for both models to reach steady state. Because of the nonlinear event of thermal runaway, we allowed the time-dependent solver to automatically determine the step size depending on the temporal gradients.

### III. MODEL WITH NO FLUID FLOW

For the first model, we do not consider fluid motion in regions 2 and 4, and only solve (1) and (4) to get steady-state temperature pattern. That way, we get a power response curve as we plot an average steady-state temperature against the incident power density of the EM waves.

In order to validate the model, we compare our power response curve with the one produced by the analytical approach introduced in [10]. We see in Fig. 2 (a) that the curves do not match precisely, but, these differences are similar to the ones discussed in [11]. Analytical model of [10] assumes uniform temperature in the X-direction, whereas the COMSOL model considers spatial variation of temperature. Biot number,  $Bi$ , is a non dimensional parameter that measures thermal losses to the surrounding. Higher the  $Bi$ , the higher is the spatial variation in temperature. As  $Bi \rightarrow 0$ , we can expect a temperature profile in the COMSOL model to become spatially uniform. From Fig. 2 (b), we see that as  $Bi$  decreases from 0.3 to 0.03, both power response curves match closely. It may not be possible to get power response curve for  $Bi = 0$  because thermal losses are zero when  $Bi = 0$ , therefore, temperature may keep on increasing with time and we may never be able

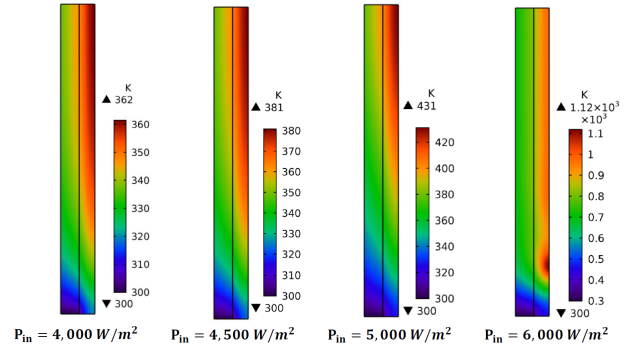


Fig. 3. Steady-state Temperature profiles as a function of  $P_{in}$  when Darcy flow is considered,  $Bi = 0.3$  and  $\Delta P = 1$  Pa.

Table 2. Power absorbed by the fluid when  $Bi = 0.3$

$P_{in}$ [ $W/m^2$ ]	$\Delta P$ [Pa]	$P_{abs}$ [ $W/m^2$ ]	$\chi$ [%]
4,000	1	206.97	0.17
4,500	1	271.70	0.2
5,000	1	436.44	0.28
6,000	1	2265.89	1.24

to reach equilibrium state. Thus, from this comparison we conclude that both the curves are in satisfactory agreement.

### IV. MODEL WITH DARCY FLOW

We consider a simplest scenario for fluid flow through porous medium as a large solid matrix and small pores of a uniform diameter, and assume that fluid motion in the pore space is represented by the Darcys law. Therefore, in addition to (1) and (4), we also solve (2) and (3), and visualize steady-state temperature profiles.

From Fig. 3, we see that, as the power density of incident EM waves increases, outlet temperature of the fluid also increases. As soon as maximum temperature reaches a critical value (at which thermal runaway initiates), we observe significant rise in fluid outlet temperature as we achieve transition between lower and middle branch of the double S-curve. It means that the total thermal energy absorbed by the fluid is much higher when we achieve transition between lower and middle branch. On the other hand, the absorbed power density, which is the rate at which the thermal energy absorbed by the fluid per unit cross sectional area, is dependent on the fluid velocity, and is given by

$$P_{abs} = (\rho C_p)_f |\vec{V}| \frac{1}{l_1} \left[ \int_0^{l_1} T_{out} dx - \int_0^{l_1} T_{in} dx \right], \quad (6)$$

where  $|\vec{V}|$  is magnitude of the velocity vector, and  $T_{out}$  and  $T_{in}$  are spatially varying temperature profiles at the outlet and the inlet, respectively. Overall thermal efficiency of the EMHE is given by

$$\chi = \theta \frac{l_1 P_{abs}}{L P_{in}}. \quad (7)$$

From (6) and (7), we calculate  $P_{abs}$  and  $\chi$  for incident power levels shown in Fig. 3, and results are tabulated in Table 2. We see that even though the fluid absorbs significant amount

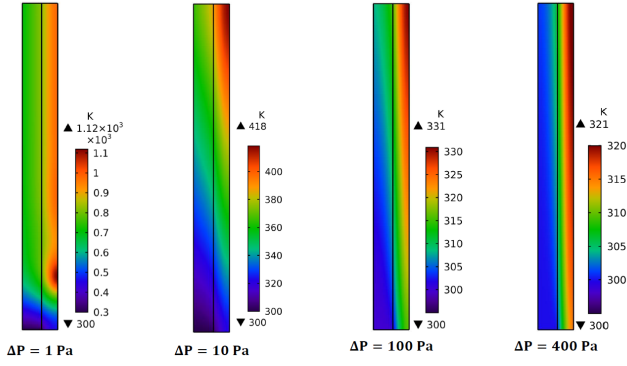


Fig. 4. Steady-state temperature profiles as a function of  $\Delta P$  when Darcy flow is considered, and  $Bi = 0.3$  and  $P_{in} = 6,000 \text{ W/m}^2$ .

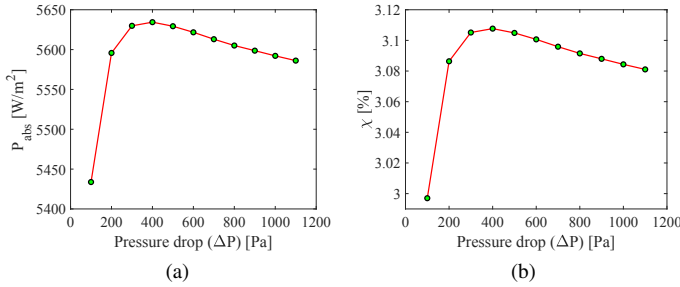


Fig. 5.  $P_{abs}$  (a) and  $\chi$  (b) as a function of pressure drop ( $\Delta P$ ) along the Y-direction for  $Bi = 0.3$ ,  $P_{in} = 6,000 \text{ [W/m}^2]$ .

thermal energy when EMHEs operate on the middle branch, the rate of energy absorption is highly dependent on how fast fluid is moving through the pores.

We now keep the incident power density of EM waves constant and vary the pressure drop ( $\Delta P$ ) across the porous media channels. The higher the  $\Delta P$ , the higher the fluid velocity ( $|\vec{V}|$ ). Steady-state temperature profiles for this scenario are shown in Fig. 4, and  $P_{abs}$  and  $\chi$  are shown in Fig. 5. We again notice that (when  $\Delta P = 1 \text{ Pa}$ ), even when outlet temperature of the fluid is significantly high, the rate at which the fluid absorbs the thermal energy is much smaller as fluid is moving very slowly.

From Fig. 5, we notice that when  $\Delta P$  increases, both  $P_{abs}$  and  $\chi$  increase because fluid velocity increases. On the other hand, when  $\Delta P$  increases even further, fluid velocity also increases but temperature gained by the fluid becomes negligible, therefore, we see decline in  $P_{abs}$  and  $\chi$ . These results show that there exists a trade off between how fast the fluid is moving in the porous medium and total thermal energy absorbed by the fluid.

## V. CONCLUSION

We have described the first 2D numerical model of porous-media-based triple layer electromagnetic heat exchanger. The developed power response curve is then validated by its comparison with the one produced by an analytical approach (for the case of no fluid flow). After the validation, we introduced Darcy flow in porous medium as a mean of collecting thermal

energy from the heat exchanger. The net power absorbed by the fluid flowing in the porous media is found to be mainly dependent on fluid velocity and outlet temperature. When the considered EMHE operates on the middle branch, total thermal energy absorbed by the fluid is significantly high but overall thermal efficiency of the device is low since the fluid is moving slowly in the porous medium.

The model discussed in this work results in inefficient operation due to the limitation that the fluid velocity is very small. Another factor affecting the overall thermal efficiency may include high thermal losses to the surrounding. The porous media based triple layer EMHE may operate efficiently if both outlet temperature and velocity of the fluid are high. The results shown in this work open up opportunities to determine optimum operating conditions and geometrical parameters of the EMHE.

## ACKNOWLEDGMENT

The authors are grateful for the support from the Air Force Office of Scientific Research; Award FA9550-15-0476 and FA9550-18-1-0528.

## REFERENCES

- [1] B. Jawdat, B. Hoff, M. Hilario, A. Baros, P. Pelletier, T. Sabo, and F. Dynys, Composite ceramics for power beaming, In *2017 IEEE Wireless Power Transfer Conference*, 978-1-5090-4595-3/17.
- [2] G.A. Landis, Beamed energy propulsion for practical interstellar flight, *J. of the British Interplanetary Society*, vol. 52, pp. 420–423, 1999.
- [3] R.M. Manning, *Beamed-Energy Propulsion: Considerations for Beaming High Energy-Density Electromagnetic Waves Through the Atmosphere*, NASA Glenn Research Center, NASA/TM-2015-218726, E-19061, GRC-E-DAA-TN21311, 2015, 58 p.
- [4] X. Wu, *Experimental and Theoretical Study of Microwave Heating of Thermal Runaway Materials*, Ph.D. Thesis, Virginia Polytechnic Institute and State University, 2002.
- [5] M. Chandran, V. Neculaes, D. Brisco, S. Katz, J. Schoonover, and L. Cretegn, Experimental and numerical studies of microwave power redistribution during thermal runaway, *J. of Applied Physics*, vol. 114, no. 20, 204904, 2013.
- [6] V.V. Yakovlev, S.M. Allan, M.L. Fall, and H.S. Shulman, Computational study of thermal runaway in microwave processing of zirconia, *Microwave and RF Power Applications*, J. Tao, Ed., Cépaduès Éditions, 2011, pp. 303–306.
- [7] G.A. Kriegsmann, Thermal runaway in microwave heated ceramic: a one-dimensional model, *J. of Applied Physics*, vol. 71, no. 4, pp. 1960–1966, 1992.
- [8] J.A. Pelesko, G.A. Kriegsmann, Microwave heating of ceramic laminates, *J. of Engineering Math.*, vol. 32, no. 1, pp. 1–18, 1997.
- [9] G.A. Kriegsmann and B.S. Tilley, Microwave heating of laminate panels, *J. of Engineering Mathematics*, vol. 44, no. 2, pp. 173–198, 2002.
- [10] J.M. Gaone, B.S. Tilley, and V.V. Yakovlev, Electromagnetic heating control via high-frequency resonance of a triple-layer laminate, *J. of Engineering Mathematics*, vol. 114, no. 1, pp. 65–86, 2019.
- [11] A.A. Mohekar, J.M. Gaone, B.S. Tilley, and V.V. Yakovlev, A 2D coupled electromagnetic, thermal and fluid flow model: Application to layered microwave heat exchangers, In *IEEE MTT-S Intern. Microwave Symp. Dig. (Philadelphia, PA, June 2018)*, pp. 1389–1392.
- [12] A.A. Mohekar, *Computational Modeling of Triple Layered Microwave Heat Exchanger*, M.S. Thesis, Worcester Polytechnic Institute, 2018.
- [13] J. Bear, *Dynamics of fluids in porous media*, Courier Corporation, 2013.
- [14] A. Sihvola, *Electromagnetic mixing formulas and applications*, IET, 1999.